DOE Cover Page

Project Title:	Development of theory and experimental operational framework for Coherent Thomson Scattering
Lead PI/Institution:	Alexandros Gerakis/Texas A&M Engineering Experiment Station
Street Address/City/State/Zip:	701 Ross street/College Station/TX/77843
Postal Address:	701 H.R. Bright Building, College Station, TX, 77843 – 3141
Collaborator:	Mikhail Shneider Princeton Collaborative Low Temperature Plasma Research Facility (PCRF)
DOE Award Number:	**DE-SC0021183**
DOE/SC Program Office:	Fusion Energy Sciences
Report Number:	DOE-TAMU-21183

Development of theory and experimental operational framework for Coherent Thomson Scattering

Final Technical Report

PI: Alexandros Gerakis
Department of Aerospace Engineering, Texas A&M Engineering Experiment Station,
College Station, TX, 77843

Table Of Contents

1 Review of Relevant Literature **2**
1.1 State of the art in plasma diagnostics: Mechanical Probes 2
1.2 State of the art in plasma diagnostics: Laser Diagnostics 2

2 Coherent Thomson Scattering **2**
2.1 From CRBS to CTS 2
2.2 Simulation of CTS 3

3 Results **5**

4 Outlook **6**

5 Products **7**

6 References Cited **8**

Abstract

The research carried out explored and proved the feasibility and operational framework of a new diagnostic technique termed Coherent Thomson Scattering (CTS) for electrons in a low temperature plasma. The work is performed in collaboration with the Princeton Collaborative Research Facility (PCRF) at Princeton Plasma Physics Laboratory. The novel technique builds on an established and demonstrated single shot diagnostic method, called Coherent Rayleigh-Brillouin scattering, which has successfully been applied in neutral flows. The proposed novel four wave mixing diagnostic technique of CTS will allow for higher spatial resolution and lower detectable number densities for the electrons than conventional Thomson scattering. In this project we developed the theoretical framework for Coherent Thomson Scattering as well as the specification of the appropriate operational experimental parameters for successful CTS implementation in e.g. a low temperature plasma. Additionally, the mode of operation and the detection limits for a practical CTS experimental demonstration were explored. Ultimately, successful experimental demonstration of CTS can be seen as transformative in a multitude of plasma physics areas, since it will allow for detailed, non-perturbative measurements of electron density and temperature, previously unattainable by other measurement techniques. This project was the first successful step towards this direction.

Acknowledgment

This work was partially supported by the Princeton Collaborative Research Facility (PCRF) and supported by the U.S. Department of Energy (DOE) under Contract No. DE-AC02–09CH11466. A.G. also received support from the U.S. DOE Office of Science Award No. DE-SC0021183.

Development of theory and experimental operational framework for Coherent Thomson Scattering.

PROJECT DESCRIPTION

Classical Thomson scattering in plasma is a standard experimental diagnostic tool used to measure density and temperature of plasma under real conditions. This technique relies on the scattering of the electromagnetic radiation from the fluctuations of electron and ion densities. However, these fluctuations produce weak, incoherent and undirected scattering signal, so that low density plasma state is hard to probe.

One of the approaches to overcome the difficulty is to make the scattering signal coherent. For this purpose, periodic perturbations of the plasma density may be initially induced by traveling optical lattice and then the probe laser beam may be scattered from these perturbations. Such a four-wave mixing scheme was applied successfully for Raleigh and Brillouin scattering diagnostics of neutral gases in the form of single shot coherent Rayleigh-Brillouin scattering (CRBS) [1–3]. In this project, drawing the analogy between neutral species and electrons, we calculate the profile of the coherent Thomson scattering signal for electron gas perturbed by a traveling optical lattice. We assume that the period of the optical lattice λ_T is much lower than the Debye length r_D, $\lambda_T << r_D$. This allows one to exclude from consideration collective plasma oscillations and waves generated due to the build-up a large space charge and formation of the self-consistent electric field in plasma. The creation of plasma waves by two counter propagating laser beams is discussed in detail in Refs. [4, 5]. The study of the scattering of the probe beam from electron and ion perturbations induced by these waves in the case of $\lambda_T << r_D$ is not examined here, and is postponed to future work.

The research conducted in this project explores the feasibility of, as well as the experimental operational framework of, a new diagnostic technique termed Coherent Thomson Scattering (CTS), for electrons in low temperature plasma conditions. This technique builds on the combined, demonstrated and established experimental and theoretical expertise that the PI has for a similar technique applicable to neutrals, termed single shot Coherent Rayleigh-Brillouin scattering. We suggest the development of a novel, four wave mixing diagnostic technique in which the resulting Thomson scattered signal beam will be another laser beam, thus allowing for higher spatial resolution and lower detectable number densities for the electrons.

In this project we developed the theoretical framework for Coherent Thomson Scattering as well as the specification of the appropriate operational experimental parameters for successful CTS implementation in a low temperature plasma. Additionally, the mode of operation and the detection limits for a practical CTS experimental demonstration were explored. Ultimately, successful experimental demonstration of CTS can be seen as transformative in a multitude of plasma physics areas, since it will allow for detailed, non-perturbative measurements, previously unattainable by any other measurement technique.

PI Gerakis collaborated with Dr. Mikhail Shneider of the Princeton Collaborative Research Facility (PCRF) at the Princeton Plasma Physics Laboratory (PPPL), to lay out the theory and experimental parameter space for CTS.

1 Review of Relevant Literature

1.1 State of the art in plasma diagnostics: Mechanical Probes

Standard mechanical probes used for the measurement of electron temperature, such as the Langmuir [6] and emissive [7] probes, significantly perturb the field to be measured and often will not survive the harsh environment they are being exposed to. These mechanical probes have the advantages of being relatively easy and inexpensive to use, they exhibit high measurement repetition rate, there exists good technical and theoretical know-how in their operation, construction and data analysis, while they are readily available through commercial suppliers. The biggest disadvantages of mechanical probes come from the fact that they are mechanical and thus finite in size: they obstruct the plasma which they aim to measure, hence altering the measurement.

1.2 State of the art in plasma diagnostics: Laser Diagnostics

The advent of lasers in 1960 [8] and the further improvement of laser technology up until today, has provided with novel, non-mechanical, generally non-intrusive techniques for the study and characterization of plasmas. For the standoff measurement of electron density and temperature in plasmas, the most dominant laser based technique is Thomson scattering, with significant applications to both high [9, 10] and low temperature plasmas [11, 12].

Thomson scattering is the result of the scattering of photons from free electrons [13, 14]. When plasma is illuminated with a laser having a narrow linewidth, the resulting Thomson scattering spectrum reveals the motion of the electrons due to Doppler shift of the scattered laser light. As such, it can reveal the electronic density since the scattering process is a linear process. Thomson scattering is analogous to Rayleigh scattering from neutral atoms and molecules, however, since the electrons have a mass thousands of times lower than atoms and molecules, the resulting Thomson scattering spectrum is orders of magnitude greater than the Rayleigh spectrum. This wide spectral characteristic has limited the application of Thomson measurements due to background interference from rotational Raman scattering, Rayleigh scattering and inherent plasma luminosity; approaches to overcome these background contributions include the use of molecular filters [15]. Moreover, since the Thomson signal is scattered in a 4π solid angle, signal acquisition in an optically noisy environment (e.g. when plasma is present) is challenging. Additionally, Thomson scattering cross-sections for electrons are wavelength independent, while for Rayleigh scattering there is a $\propto \lambda^{-4}$ dependence with wavelength, where λ is the wavelength of the illuminating laser. Due to the low cross-sections for Thomson scattering from electrons, highly energetic lasers (on the order of $1.5-2$ Joules/pulse over ~ 8 ns pulse duration at 10 Hz repetition rate) [16–18] are usually employed to perform the measurement. Finally, in Thomson scattering the signal is collected in a line integrated mode, thus resulting in a relatively low spatial resolution for the technique [19]. Increased spatial resolution for Thomson scattering has been demonstrated in Reference 20, where the Thomson scattering beam is incident at the Bragg angle on inherent plasma waves in the device, thus resulting in a localized measurement, as discussed in Section 2.1.

2 Coherent Thomson Scattering

2.1 From CRBS to CTS

CRBS relies on the electrostrictive force to attract neutral particles to the high intensity nodes of the created interference pattern thus resulting in an optical lattice. Only particles with a velocity

v, equal (or close to equal) to the velocity of the lattice v_g can follow its movement and populate the lattice sites. This mechanism is key to the proposed concept of CTS.

Assuming a weakly ionized plasma, neutrals, ions and electrons will be present in the vicinity of the optical interference pattern. If the lattice velocity is increased to values exceeding those of the neutral and ionic velocity distribution functions (VDFs), then only electrons (whose VDF is much wider than those of the ions and the neutrals) will populate the lattice sites. In this case, the signal will be dominated by the electronic contribution, giving rise to Coherent Thomson Scattering. The physics of our proposed concept is not dissimilar to that demonstrated in Ref. 20 in which a laser beam was scattered off from waves naturally occurring in the plasma. The key difference between the two approaches though is that with the approach proposed here electronic waves are induced with the pump beams, hence rendering the CTS technique to be applicable to a multitude of plasmas. Additionally, similarly to the spatial resolution exhibited with CRBS, CTS provides with increased spatial resolution which many of the current Thomson scattering diagnostics are lacking.

2.2 Simulation of CTS

The intensity of scattering signal is determined by the Bragg reflection coefficient R of the probe beam, $R \approx 2N^2(\Delta n)^2(\lambda_L/\lambda)^2$, where N is number of periods in the optical lattice, Δn is the perturbation of the refraction index for the probe laser beam having a wavelength λ and λ_L is period of the optical lattice. With the contribution due to ions neglected, the steady-state perturbation Δn is related to electron density modulation Δn_e induced by the optical lattice $\Delta n = -\frac{1}{2}\omega_p^2\omega^{-2}\Delta n_e/n_e$ where ω_p is the plasma frequency and ω is the probe beam frequency. The intensity of the scattered signal I in a relative units is proportional to the electron density perturbation squared, $I \sim \left(\Delta n_e\right)^2$.

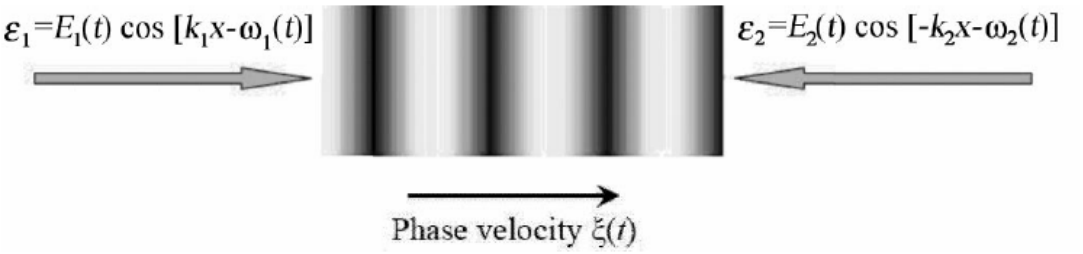

Figure 1: The creation of an optical lattice by two counter-propagating optical fields

The optical lattice to induce the electron density perturbations is formed by two counter- propagating laser beams having wave vectors k_1 and k_2 with frequencies ω_1 and ω_2 close to each other, $\omega_1 \approx \omega_2 \approx \omega$. (see Fig. 1).The mechanical motion of an electron is controlled by an optical gradient force F_{pond}. Let the crests and valleys of the lattice be along the x-axis and denote $k_{1\chi}$ and $k_{2\chi}$ the projections of the vectors k_1 and k_2 on x-axis. If the phase velocity of the lattice $\xi = (\omega_1 - \omega_2)/(k_{1\chi} + k_{2\chi})$ is not zero, the force $F_{pond} = -e^2E_{01}/\left(2m\omega^2\right)\frac{\partial}{\partial x}[cos\,(\Omega t + qx)]$, where e is the electron charge, E_{01} and E_{02} are the electric fields in the two laser waves, m is the electron mass, $\Omega = \omega_1 - \omega_2$ and $q = (k_{1\chi} + k_{2\chi})$. In the limit $\xi = 0$ and with $E_0 = E_{01} = E_{02}$, the two laser beams produce a standing wave, and in this case the optical gradient force averaged over time is given by $F_{pond} = -e^2E_0^2/\left(2m\omega^2\right)\frac{\partial}{\partial x}cos\,(kx))$, where $k = k_{1\chi} = -k_{2\chi}$.

As an example, we consider a one-component weakly ionized argon plasma with low electron and ion n_i densities, which are equal to each other, $n_e \approx n_i \approx 10^{10}-10^{11}$ cm^{-3}, electron temperature $T_e = 1$ eV , the cold argon atoms having density 6.6×10^{17} cm^{-3} and temperature T= 293 K . Collisions between charged particles are totally ignored and those between electrons and neutrals are assumed to be relatively rare, so that an electron mean free pass l is greater than the lattice period λ_L. Actually, for the conditions mentioned above, we have $\tau = 10^{-11}$s and the electron mean free path $l \approx 7 \times 10^{-4} cm$, which is 25 times higher than the period of the optical lattice $\lambda_T = \lambda/2 = 2.66 \times 10^{-5}$ cm, the lattice being created by the two identical counter propagating laser beams with wavelength $\lambda_T = 532nm$.

Thus, to determine Δn_e due to the force F_{pond} a kinetic approach is required. We assume that the ions form a fixed neutralizing background. A kinetic equation for $1D-1V$ electron distribution function $f = f(x, \upsilon, t)$ has the form:

$$\frac{\partial f}{\partial t} + \upsilon \frac{\partial f}{\partial x} + \left(\frac{F_{pond} - eE}{m} \right) \frac{\partial f}{\partial \upsilon} = -\frac{f - f_0}{\tau}. \tag{1}$$

Here, the right hand side is a Bhatnagar-Gross-Krook term, which describes the collisions between electrons and neutrals, τ is the characteristic time between the collisions, $f_0 = 1/\sqrt{2\pi}\upsilon_{eT} \exp(-\upsilon^2/\upsilon_{eT}^2)$ is the Maxwellian electron distribution function, $\upsilon_{eT} = \sqrt{kT_e/m}$ is the characteristic electron thermal velocity and E is the self-consistent electric field that establishes due to the shift of the electrons with respect to immobile ions. Eq. 1 is supplemented by the Poisson equation for the electric field E:

$$\frac{\partial E}{\partial x} = \frac{\rho}{\varepsilon_0}, \rho(x,t) = e\left(n_i - \int f(x, \upsilon, t)\, d\upsilon \right) \tag{2}$$

where ρ is the density of space charge.

To find Δn_e, we need to solve the initial value problem 1 - 2 with the initial conditions $f(x, \upsilon, t = 0) = f_0$ and $E(x, t = 0) = 0$. The phase velocity of the lattice $\xi = \Omega/q$ serves as an input parameter, which is varied from ≈ 0 to $\xi \approx 3.5\upsilon_{eT}$. We assume that the counter - propagating laser beams are practically identical; thus we have $E_0 = E_{01} = E_{02}$ and $q = k_{1\chi} + k_{2\chi} = 2k = 4\pi/\lambda$ in the expression for the force F_{pond}. The computational domain in (x, υ) space consists of a segment $[0, \lambda_T]$ along the x-direction, covering one period of the optical lattice λ_T, and of a segment $[-5\upsilon_{eT}, 5\upsilon_{eT}]$ in the u - direction. Eq. 1 is solved numerically by LeVeque's insplit wave propagation method [21]. As in [22], Eq. 2 is transformed to the current conservation equation and solved by explicit scheme. The periodic boundary conditions for electron distribution function $f(0, \upsilon, t) = f(\lambda_T, \upsilon, t)$ and electric field $E(0, t) = E(\lambda_T, t)$ are employed. At a given velocity of the lattice $\xi = \Omega/q$ we calculate $f(x, \upsilon, t)$ up to the steady state. The time required for the steady state to establish is no longer than 10^{-10} seconds. The computed stationary value of $f(x, \upsilon, t)$ gives the relative perturbation of the electron density $(\Delta n_e)^2 = \int_0^{\lambda_T} dx \left[\int_{-\infty}^{+\infty} (f(x, \upsilon, t) - f_0(\upsilon, 0)) d\upsilon \right]^2$ for each ξ and thus a scattered signal.

3 Results

At low intensity of the pump lasers, $I = 10^9$ W/cm^2, the perturbations induced by the optical lattice are small, and the scattering spectral profile corresponds to the Maxwellian electron distribution function taken initially (see Fig. 2a). When increasing the pump intensity from up to I = 10^{12}W/cm^2, the spectral profile first gradually narrows and then its width does not decrease any longer with I (Fig. 2b).

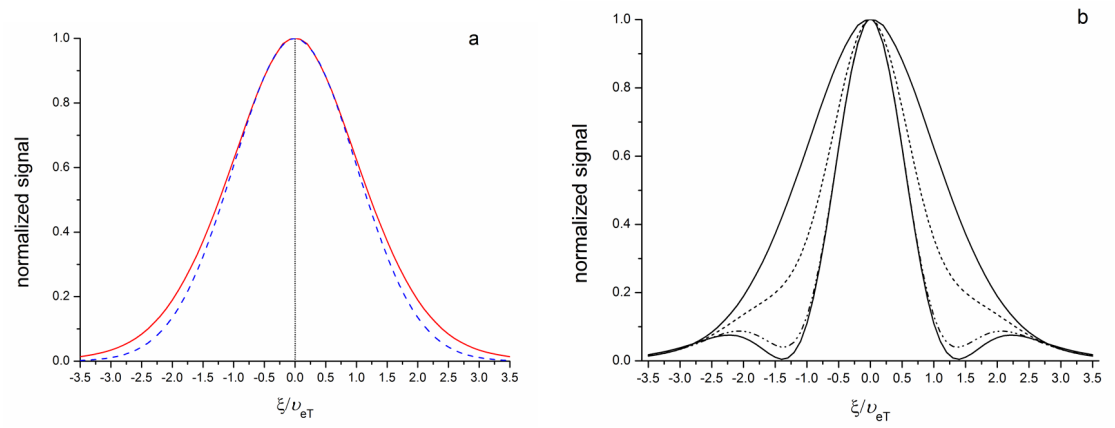

Figure 2: a) Coherent Thomson scattering spectral profile from electron gas with $T_e = 1$ eV at the pump intensity $I = 10^9$ W/cm^2 vs the phase velocity of the optical lattice. Also shown is the Doppler profile of spontaneous Thomson scattering from electron gas (dashed blue line) and that from neutral argon gas with temperature T=293 K (dotted line); (b) A comparison between calculated coherent Thomson scattering spectral profile from electron gas at pump intensities $I = 10^9$ (broad solid line) and 10^{12} W/cm^2 (narrow solid line). Also shown are the calculated spectral profiles from electron gas at $I = 10^{10}$ W/cm^2 (dashed line) and at $I = 10^{11}$ W/cm^2 (dashed-dotted line).

An analogous narrowing of the spectral profile at the high pump intensities was predicted and observed in neutral gas [23, 24]. When the narrowing occurs, the perturbations of the electron distribution function due to optical force become noticeable. This is illustrated in Fig. 3.

Finally, it is interesting to compare the intensity of the discussed coherent scattering with that of incoherent scattering. For this purpose we should compare the Bragg reflection coefficient R with the value $\sigma_T n_e V/\left(4^2\right)$, where $\sigma_T = 6.65 \times 10{-}25$ cm^2 is the Thomson scattering cross-section, V is the scattering volume and r is the distance from the plasma source. Assuming the scattering volume to be cylindrical in shape with length L= 0.1 cm and diameter D= 100μm and the distance $r = 1$ m, for the electron density $n_e = 10^{11}$ cm^{-3}, we have $\sigma_T n_e V/\left(4\pi r^2\right) = 4.2 \times 10^{24}$. On the other side, from numerical simulations, we have the relative change of the electron density due to optical lattice at pump intensity $I = 10^{11}$ W/cm^2 to be $\Delta n_e/n_e \approx 10^{-3}$.

For the perturbation of refraction index, we have $\Delta n = -\frac{1}{2}\frac{\omega_p^2}{\omega^2}\frac{\Delta n_e}{n_e} = 1.3 \times 10^{-14}$. Thus, with an optical lattice of 1 cm in length, having approximately $N = 3.810^4$ periods the reflection coefficient $R \approx 10^{-19}$. This value is almost five orders of magnitude higher than that the above value 4.2×10^{-24} obtained for a spontaneous Thomson scattering signal.

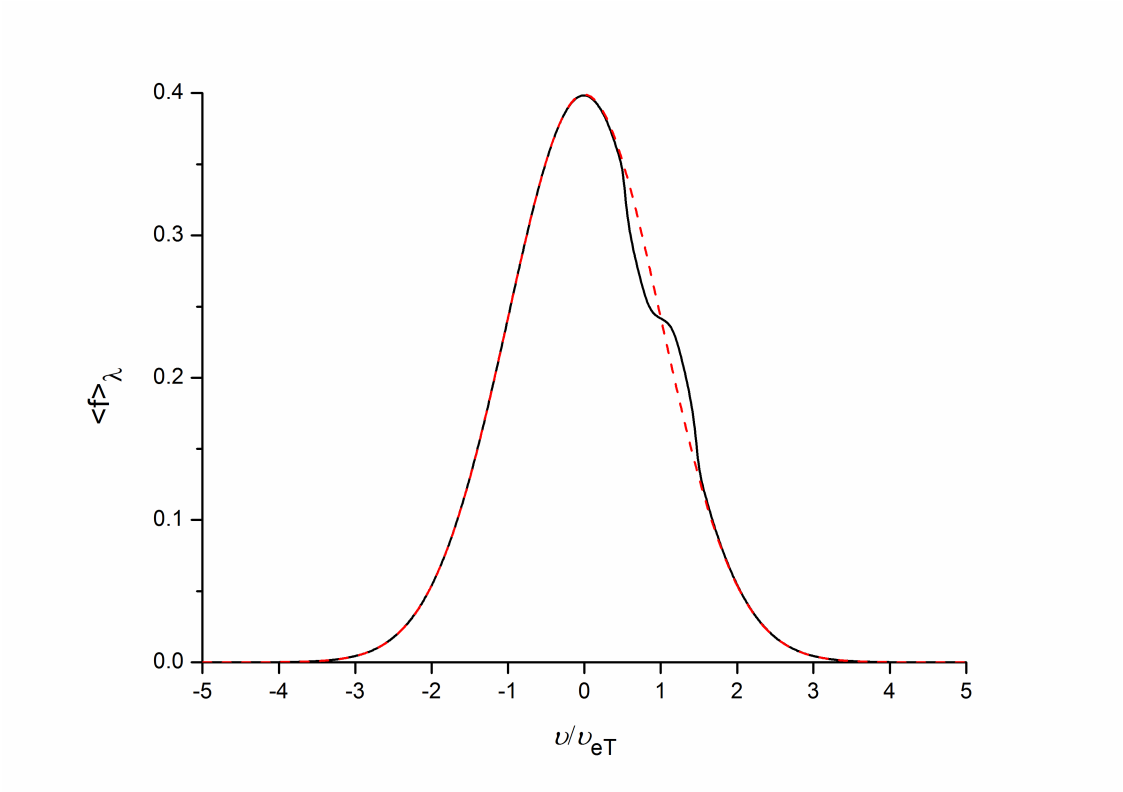

Figure 3: The steady-state perturbation of electron velocity distribution function by a pulsed optical lattice moving with velocity $\xi = 4.19 \times 10^7$ cm s^{-1}. The distribution function is averaged over the lattice period. The pump intensity is $I = 10^{12}$ W/cm^2 ; $T_e = 1$ eV. The dotted line is the initial Maxwellian distribution function.

4 Outlook

At the core, the proposed four-wave mixing Thomson scattering scheme is the utilization of optical lattices for the creation of the periodic perturbation of electron density in plasmas via a periodic optical dipole force. The traveling optical potential perturbs the motion of a group of electrons whose velocities are close to the speed of the interference pattern of the crossed pump fields. By changing the frequency difference between the two pump laser beams, or the speed of the interference pattern, a perturbation of electron distribution function centered at the particular velocity is created. The relative magnitude of the induced electron density perturbation at each velocity can be determined by the measurement of the relative intensity of a third probe laser beam, Bragg scattered from the induced electron density perturbations.

This scheme is capable of by-passing the Rayleigh signal contributions from neutrals and ions in the plasma — only keeping the Thomson scattering signal from the electrons. More importantly, this scheme results in a coherent Thomson signal beam, which maintains all the beam characteristics of the probe beam. This enables the placement of the collection optics far from the point of measurement without any loss of signal, in comparison with, for example, incoherent Thomson scattering where the signal scales with $1/r^2$ with respect to the distance r where the collection optics are placed. It is envisioned that this capability will enable accurate and non-intrusive measurements

in low-density plasmas, where the current state-of-the-art is mechanical probes.

The four-wave mixing nature of the proposed technique renders it ideal for application in optically noisy environments, such as those encountered in plasmas—while the necessary angled crossing of the laser beams provides with a high degree of localization and spatial resolution. Furthermore, if one utilizes a chirped lattice approach, where the range of optical lattice velocities is scanned in a single laser shot (as experimentally demonstrated and theoretically studied for neutral gases in Ref. [25]), it is envisioned that the induced coherent Thomson scattering scheme will have single shot spectral acquisition, making it an ideal diagnostic for highly dynamic systems. As the next phase towards these directions, we will actively pursue the experimental demonstration of coherent Thomson scattering in a low temperature plasma environment.

5 Products

The results of this project have resulted in one publication in a peer-reviewed journal:

Mikhail Mokrov, Mikhail N. Shneider, and Alexandros Gerakis , "*Analysis of coherent Thomson scattering from a low temperature plasma*", Physics of Plasmas 29, 033507(2022)

The results of this project will be presented in two conferences:

- APS Gaseous Electronics Conference 2022
- APS Division of Plasma Physics Meeting 2022

6 References Cited

[1] Gerakis, A., Shneider, M. N., and Stratton, B. C., "Remote-sensing gas measurements with coherent Rayleigh-Brillouin scattering," *Applied Physics Letters*, Vol. 109, No. 3, 2016, pp. 31112.

[2] Gerakis, A. and Shneider, M. N., "Gas flow velocity and density limit estimates for single shot coherent Rayleigh-Brillouin scattering," *AIAA Scitech 2020 Forum*, 2020, p. 0520.

[3] Gerakis, A., Coppendale, N., Maher-McWilliams, C., Douglas, P., and Barker, P. F., "A high-energy chirped laser system for fast manipulation of gases," *Conference on Lasers and Electro-Optics 2012*, Optical Society of America, 2012, p. QW3E.4.

[4] Kroll, N. M., Ron, A., and Rostoker, N., "Optical Mixing as a Plasma Density Probe," *Phys. Rev. Lett.*, Vol. 13, Jul 1964, pp. 83–86.

[5] Michel, P., Rozmus, W., Williams, E. A., Divol, L., Berger, R. L., Glenzer, S. H., and Callahan, D. A., "Saturation of multi-laser beams laser-plasma instabilities from stochastic ion heating," *Physics of Plasmas*, Vol. 20, No. 5, 2013, pp. 056308.

[6] Langmuir, I., "The pressure effect and other phenomena in gaseous discharges," *Journal of the Franklin Institute*, Vol. 196, No. 6, 1923, pp. 751 – 762.

[7] Sheehan, J. P. and Hershkowitz, N., "Emissive probes," *Plasma Sources Science and Technology*, Vol. 20, No. 6, nov 2011, pp. 063001.

[8] Maiman, T. H., "Stimulated optical radiation in ruby," *nature*, Vol. 187, No. 4736, 1960, pp. 493–494.

[9] Peacock, N., Robinson, D., Forrest, M., Wilcock, P., and Sannikov, V., "Measurement of the electron temperature by Thomson scattering in tokamak T3," *Nature*, Vol. 224, No. 5218, 1969, pp. 488–490.

[10] Murmann, H., Götsch, S., Röhr, H., Salzmann, H., and Steuer, K. H., "The Thomson scattering systems of the ASDEX upgrade tokamak," *Review of Scientific Instruments*, Vol. 63, No. 10, 1992, pp. 4941–4943.

[11] Muraoka, K. and Kono, A., "Laser Thomson scattering for low-temperature plasmas," *Journal of Physics D: Applied Physics*, Vol. 44, No. 4, jan 2011, pp. 043001.

[12] van der Meiden, H. J., Al, R. S., Barth, C. J., Donné, A. J. H., Engeln, R., Goedheer, W. J., de Groot, B., Kleyn, A. W., Koppers, W. R., Lopes Cardozo, N. J., van de Pol, M. J., Prins, P. R., Schram, D. C., Shumack, A. E., Smeets, P. H. M., Vijvers, W. A. J., Westerhout, J., Wright, G. M., and van Rooij, G. J., "High sensitivity imaging Thomson scattering for low temperature plasma," *Review of Scientific Instruments*, Vol. 79, No. 1, 2008, pp. 013505.

[13] Thomson, J. J., "On Electrical Oscillations and the effects produced by the motion of an Electrified Sphere," *Proceedings of the London Mathematical Society*, Vol. 1, No. 1, 1883, pp. 197–219.

[14] Tanenbaum, B. S., "Continuum Theory of Thomson Scattering," *Phys. Rev.*, Vol. 171, Jul 1968, pp. 215–221.

[15] Zaidi, S. H., Tang, Z., Yalin, A. P., Barker, P., and Miles, R. B., "Filtered Thomson Scattering in an Argon Plasma," *AIAA Journal*, Vol. 40, No. 6, 2002, pp. 1087–1093.

[16] Rozenblat, R., Kolemen, E., Laggner, F. M., Freeman, C., Tchilinguirian, G., Sichta, P.,

and Zimmer, G., "Development of Real-Time Software for Thomson Scattering Analysis at NSTX-U," *Fusion Science and Technology*, Vol. 75, No. 8, 2019, pp. 835–840.

[17] Zweben, S. J., Myra, J. R., Diallo, A., Russell, D. A., Scotti, F., and Stotler, D. P., "Blob wakes in NSTX," *Physics of Plasmas*, Vol. 26, No. 7, 2019, pp. 072502.

[18] Diallo, A., Dominski, J., Barada, K., Knolker, M., Kramer, G. J., and McKee, G., "Direct Observation of Nonlinear Coupling between Pedestal Modes Leading to the Onset of Edge Localized Modes," *Phys. Rev. Lett.*, Vol. 121, Dec 2018, pp. 235001.

[19] LeBlanc, B. P., Diallo, A., Labik, G., and Stevens, D. R., "Radial resolution enhancement of the NSTX Thomson scattering diagnostic," *Review of Scientific Instruments*, Vol. 83, No. 10, 2012, pp. 10D527.

[20] Tsikata, S. and Minea, T., "Modulated Electron Cyclotron Drift Instability in a High-Power Pulsed Magnetron Discharge," *Phys. Rev. Lett.*, Vol. 114, May 2015, pp. 185001.

[21] LeVeque, R. J., *Finite Volume Methods for Hyperbolic Problems*, Cambridge Texts in Applied Mathematics, Cambridge University Press, 2002.

[22] Horne, R. B. and Freeman, M. P., "Regular Article," *Journal of Computational Physics*, Vol. 171, No. 1, 2001, pp. 182–200.

[23] Bookey, H. T., Shneider, M. N., and Barker, P. F., "Spectral Narrowing in Coherent Rayleigh Scattering," *Phys. Rev. Lett.*, Vol. 99, Sep 2007, pp. 133001.

[24] Shneider, M. N., Barker, P., Pan, X., and Miles, R. B., "Coherent Rayleigh scattering in the high intensity regime," *Optics Communications*, Vol. 239, No. 1, 2004, pp. 205–211.

[25] Pan, X., Shneider, M. N., and Miles, R. B., "Coherent Rayleigh-Brillouin Scattering," *Phys. Rev. Lett.*, Vol. 89, Oct 2002, pp. 183001.

Analysis of coherent Thomson scattering from a low temperature plasma

Mikhail Mokrov± mmokrov@gmail.com
Institute for Problems in Mechanics, Russian Academy of Sciences, Moscow, 119526, Russia

Mikhail N. Shneider* shneyder@princeton.edu
Department of Mechanical & Aerospace Engineering, Princeton University, Princeton, NJ, 08544, USA

Alexandros Gerakis† alexandros.gerakis@list.lu
Department of Aerospace Engineering, Texas A&M University, College Station, TX, 77845, USA
Luxembourg Institute of Science & Technology, Belvaux, L-4362, Luxembourg

Abstract. The spectrum of coherent Thomson scattering (CTS) induced by a periodic ponderomotive perturbation in a low-density low temperature plasma is considered. The analysis is performed for the case when the period of the resulting optical lattice is less than the Debye screening length in the plasma by solving an electron Boltzmann equation, where the total force is the sum of the periodic force due to the optical lattice and the electrostatic force due to self-consistent electric field in the plasma. An analogy between the CTS spectra calculated here and coherent Rayleigh scattering spectra in a neutral gas is established. For relatively low intensity for the optical lattice, the calculated CTS spectra are nearly Gaussian with widths slightly wider than the incoherent Thomson widths. We demonstrate that at higher intensities the line shape narrows and saturates to a width approximately half of that found at low lattice intensities. The proportionality of the spectral width to the square root of the electron temperature allows one to extract the electron temperature from the saturated spectra. Possible application of CTS for remote measuring the electron temperature in plasma is discussed.

I. INTRODUCTION

The study of the complex behavior of the charged species in various plasma sources and devices requires substantial improvement of non-intrusive plasma diagnostic techniques. Incoherent Thomson scattering (ITS) of radio waves and laser radiation has been used for the non-invasive measurement of the electron density and temperature in plasmas from the 1960s up to today [1,2]. ITS is characterized by the scattering parameter $\alpha = (hr_D)^{-1}$, where $h = |\boldsymbol{k} - \boldsymbol{k}'|$, r_D is the Debye length, and the wave vectors $\boldsymbol{k}$ and $\boldsymbol{k}'$ describe incident and scattered waves, respectively. If $\alpha > 1$, electron fluctuations in the plasma are strongly coupled to those of ions, giving rise to the so-called 'collective' scattering. If $\alpha < 1$, the electrostatic interactions become non-important and thus the incoherent scattering due to thermal fluctuations occurs as if the charged particles are free. Laser ITS experiments in this regime have shown that the frequency of photons from a narrow linewidth laser is Doppler shifted due to the scattering from the electrons in the plasma [3,4]. In the collisionless limit, the spectrum of ITS is similar to that of the Rayleigh scattering from neutral particles [5].

However, since the electrons have a much smaller mass and their translational temperature in a low-density, low temperature plasma is usually much higher than that of heavy species, the Thomson scattering spectral linewidth is orders of magnitude broader than the Rayleigh linewidth.

ITS is mainly used for diagnostics of dense fusion plasma in state-of-the-art plasma devices [2,6–10]. In this technique, the incident probe laser power is scattered to 4π steradians, while the scattering power is proportional to the number of electrons in the scattering volume, decaying as r^{-2} with the distance r from the scattering volume. This gives rise to a low ratio of the scattered power to that of the probe laser and limits the application of ITS for diagnostics of low temperature plasma sources with electron densities of 10^{12} cm^{-3} or lower [4,11–17]. To perform ITS measurements under such low densities it is paramount to attenuate stray light, collect statistics, accumulate measurements for thousands or tens of thousands of laser pulses or significantly increase the intensity of laser radiation. These approaches are problematic, since accumulating statistics over a long time (tens of minutes or several hours) is impractical and meaningless under non-stationary plasma conditions, while an increase in laser intensity may only lead to large disturbances in the plasma under study [18].

In this paper we propose a novel, alternative approach to measuring the electron temperature and density in a low-density plasma. This approach relies on the observation of Bragg scattering or induced coherent Thomson scattering from the electron gas trapped by traveling optical lattice potentials and is a variation of four-wave mixing techniques. Following this approach, it is anticipated that the scattered signal will be largely increased, due to the constructive interference of the waves reflected from a refractive-index grating induced in a weakly ionized plasma by the ponderomotive interaction of the electron gas with an moving optical interference pattern. The resulting signal beam is another *coherent* laser beam, maintaining all the characteristics of the probe. The diagnostic scheme presented here is not to be confused with the "collective" Thomson scattering mentioned above, which is sometimes referred to as "coherent Thomson scattering" in the literature [19,20].

In the case considered here, the electron density perturbation δn_e is a traveling wave that oscillates at the beat frequency of pump beams $\Omega = \omega_1 - \omega_2$, with a grating wave vector $\boldsymbol{q} = \boldsymbol{k_1} - \boldsymbol{k_2}$, where $\boldsymbol{k_1}$ and $\boldsymbol{k_2}$ are wave numbers of two pump beams which interfere within the plasma. The value of δn_e at different beat frequencies Ω determines the intensity of the scattered signal. The character of electron density perturbation depends on the value of

parameter $(qr_D)^{-1}$, where $q = |\boldsymbol{q}|$. If $(qr_D)^{-1} > 1$, the electron density perturbations in the plasma are strongly coupled to those of ion density via self-consistent electric field in plasma [21,22]. In contrast, at $(qr_D)^{-1} \ll 1$, electrostatic interactions are weak, and the electrons are, in fact, subject only to the external optical field. Here we focus on the latter case and check the unimportance of the electrostatic interactions by direct numerical simulation. The condition $(qr_D)^{-1} \ll 1$ can be met in a plasma with a not too large electron density n_e; for example, if it is assumed that the electron temperature is $T_e = 1$ eV and the optical lattice produced by two counter-propagating laser beams has a wavelength of λ = 266 nm, then $n_e \ll 1.2 \times 10^{17}$cm^{-3}. Here, we calculate the line shape of the resulting coherent Thomson scattering signal and demonstrate that line narrowing occurs for high intensities of the pump lasers. This is in analogy to similar phenomena observed and studied in the past for atomic and molecular gases, where the four-wave mixing technique has been used to determine temperature and neutral atomic and molecular gas composition from the coherent Rayleigh and Rayleigh-Brillouin scattering line shape [23–26].

II. FORMULATION OF THE PROBLEM

Consider the motion of charged particles in an electric field of two interfering laser beams, termed the *pumps*, that cross at angle θ and have frequencies ω_1 and ω_2 and wave numbers $\boldsymbol{k_1}$ and $\boldsymbol{k_2}$. We choose the *x*-axis along the vector $\boldsymbol{q} = \boldsymbol{k_1} - \boldsymbol{k_2}$, which is perpendicular to the fringes of the optical lattice. The period of the lattice d is determined by the angle θ, $d = \lambda/[2sin(\theta/2)]$, where λ is the pump wavelength. For two almost counter-propagating ($\theta \approx \pi$) pump beams (see Fig.1), $d = \lambda/2$ and $q = 4\pi/\lambda$, where $q = |\mathbf{q}|$. In an experiment, the beams must be crossed within a plasma at an angle close to but not equal to π, to avoid backwards propagation of the laser beams. This crossing angle results in the interference pattern to be two-dimensional. However, as work in gases with the beams crossing at an angle of 178° shows, the theory based on the one-dimensional approximation describes the experiment well [23–25].

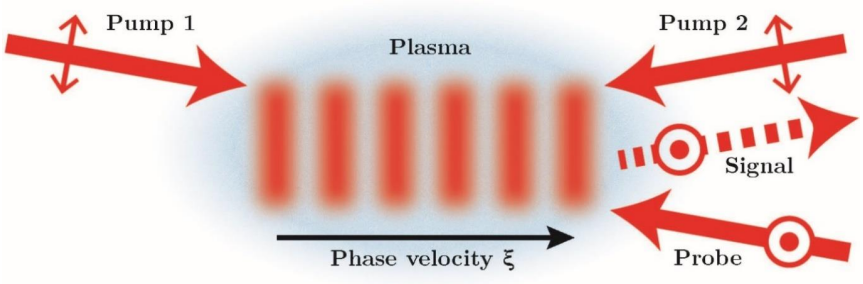

FIG. 1. The creation of an optical lattice within a plasma, by two almost counter-propagating optical beams of the same polarization. A third probe beam, of orthogonal polarization is shown at the Bragg angle on the induced electron periodic density modulation, giving rise to the four-wave mixing Thomson scattering signal beam. The probe beam's polarization is set perpendicular to that of the pump beams in order to avoid interference between the probe beam and any of the pump beams.

The electric field of the two interfering pump beams produces a traveling optical potential which moves at a phase velocity $\xi = \Omega/q$. In a weakly ionized plasma this potential will trap electrons in the low intensity nodes, due to the ponderomotive force. To induce noticeable electron density perturbations, the phase velocity ξ has to fall within the range of electron velocities v for which the value of the one-dimensional velocity distribution function (VDF) of electrons $f \propto \exp(-v^2/2v_{eT}^2)$ is significant, where $v_{eT} = \sqrt{kT_e/m}$, where T_e is the electron temperature and m is the electron mass. Similarly, the one-dimensional VDF of ions or neutral species with velocities v_h will be given by $f_h \propto \exp(-v_h^2/2v_T^2)$, where the characteristic thermal velocity now is $v_T = \sqrt{kT/M}$, where T is the species' temperature and M is their mass. Since $M >> m$, it follows that the electronic VDF will be much wider than the one for the heavy species, even if assuming that $T_e = T$. Consequently, if ξ is greater than the velocities seen in the heavy species VDF, then one cannot expect that the motion of ions and neutral particles will be greatly perturbed by the optical lattice. On the other hand, a relative shift of electrons with respect to ions in the plasma leads to the generation of a self-consistent electric field, which tends to slow down the electrons and drag the ions. However, if the charge separation occurs at a distance of about one optical lattice period which is much lower than the Debye length, then this electric field is relatively small and the motion of ions under its action can be neglected. Thus, the electrostatic field is taken into consideration to maximize its effect on the electron motion, while the ions are assumed to form a fixed neutralizing background.

An electron placed in the electric field generated by the interference of two pump beams is accelerated by the ponderomotive force $F = -\partial U(x,t)/\partial x$ with an effective optical potential $U(x,t) = \frac{e^2 E_{01} E_{02}}{2m\omega^2}\cos(\Omega t + qx)$, where e is the electron charge, E_{01} and E_{02} are the electric fields amplitudes of the two pump beams, and ω is the laser frequency, which is close to both ω_1 and ω_2; we assume that $|\Omega| = |\omega_1 - \omega_2| \ll \omega_1, \omega_2$. The formula for $U(x,t)$, which corresponds to the traveling optical potential, has been obtained by us by modifying slightly the derivation (given, for example, in [27]) of the stationary ponderomotive potential $U(x)$ for a standing light wave.

Since the mean free path of the electrons with respect to various types of collision, such as electron-neutral particle and electron-ion, is higher than the length scale of the optical force gradients (typical dimensions of $d = \lambda/2 = 266$ nm, assuming counter-propagating pump beams with a wavelength of 532 nm) the perturbation of the electron density δn_e is found by a kinetic approach. To calculate the electron distribution function $f = f(x,v,t)$, we solve the Boltzmann equation, subject to the assumption that the total force acting on electrons in the plasma is a sum of the periodic ponderomotive force F and the self-consistent electrostatic force $-eE$:

$$\frac{\partial f}{\partial t} + v\frac{\partial f}{\partial x} + \frac{(F - eE)}{m}\frac{\partial f}{\partial v} = -\frac{f - f_0}{\tau} \qquad (1)$$

Here $f_0 = 1/(\sqrt{2\pi}v_{eT})\exp(-v^2/2v_{eT}^2)$ is the Maxwellian electron distribution function, the collision integral is written in the Bhatnagar-Gross-Krook approximation [28] and τ is the characteristic time between collisions. If electron-neutral atom collisions are dominant, the relaxation time τ in (1) can be calculated as $\tau = l/v_{em}$, where $l = 1/(N\sigma_{tr})$ is the electron mean free path for electron-neutral atom collisions with gas of a density N, $v_{em} = \sqrt{8kT_e/\pi m}$ is the electron mean velocity and σ_{tr} is the effective momentum transfer cross section.

To illustrate the validity of the operating regime considered here, without loss of generality, we consider the perturbation of electron density in a quasineutral weakly ionized plasma in a gas of argon, which is at a temperature of $T = 293\ K$ and at a pressure of 216 Torr, having an electron density of $n_e = 10^{11}$ cm^{-3} at a temperature of T_e = 1–3 eV. These conditions are typical for a low-temperature plasma source. For $T_e = 1$ eV, we have $\tau = 10^{-11}$ s and $l = 6.7\times 10^{-4}$ cm, which is 25 times higher than the period of the optical lattice d=λ/2=266 nm, hence demonstrating the validity of the kinetic approach followed here.

To determine the electric field E in equation (1) self-consistently, we use the Poisson equation:

$$\frac{\partial E}{\partial x} = \frac{\rho}{\varepsilon_0}, \qquad (2)$$

where $\rho(x,t) = e(n_i - \int f(x,v,t)dv)$ is the space charge density and n_i is a fixed density of ions.

Thus, the perturbation of the electron density at each lattice phase velocity $\xi = \Omega/q$ is determined by solving the initial value problem for Eqs. (1)–(2) with the initial conditions $f(x,v,t=0) = f_0$ and $E(x,t=0) = 0$. The intensities of the two pump beams are assumed to be equal to each other $I = I_1 = I_2$. Even for the highest pump intensities considered in this paper, $I = 10^{12} - 10^{13}$ W/cm^2, we have the parameter $|U|/(kT_e) = 0.1$, so that the modification of the electron distribution function by the optical lattice is relatively small, as compared to the Maxwellian one.

The computational domain is rectangular in the (x,v) space, with the domain width along the $x-$ direction equal to the optical lattice period d. Eq. (1) is solved numerically by LeVeque's unsplit wave propagation method [29]. As in Ref. [30], Eq.(2) is transformed to the current conservation equation and solved for $E(x,t)$ by an explicit scheme. As in Refs. [31,32], the assumption of the optical potential which is one-dimensional and periodic allows the use of the periodic boundary condition $f(0,v,t) = f(d,v,t)$. The same condition is applied for the electric field $E(0,t) = E(d,t)$. In addition, we have $f(x, v\to\infty, t) = 0$. With regards to the latter condition, in the implemented numerical method we have restricted the absolute value of electron velocity to values not exceeding $5v_{eT}$. We seek the solution of Eqs. (1)–(2) for the potential $U(x,t)$ created by the pump laser field pulse with a rectangular shape and temporal width not greater than 0.1 ns.

The mean electron density perturbation squared is computed as $(\delta n_e)^2 = n_e^2 d^{-1}\int_0^d dx\left|\int_{-\infty}^{+\infty}[f(x,v,t) - f_0]dv\right|^2$ and it takes a time of the order of 10 ps for $(\delta n_e)^2$ to approach the steady state in the numerical simulations. The fact that the steady state is reached quickly confirms the initial assumption that electrostatic plasma oscillations can neglected in the case considered here. The value of $(\delta n_e)^2$ ultimately determines the scattering signal at each phase velocity of the optical lattice ξ. Indeed, the intensity of the generated signal laser beam is described by the Bragg reflection coefficient R from the periodic structure with the modulation of the refractive index δn. The refractive index δn is expressed via the electron density perturbation δn_e induced by the optical lattice, $\delta n = -\left(\omega_p/\omega_3\right)^2 \delta n_e/(2n_e)$, where ω_p is the plasma frequency and ω_3 is the frequency of

the probe beam. The reflection coefficient from such a grating with $\delta n \ll 1$ is given by $R \approx \tanh^2(\sqrt{2}\delta n K d/\lambda_3)$ [33], where $K = L/d$ is the number of periods in the optical lattice having a length L and $\lambda_3 = 2\pi c/\omega_3$. The argument of hyperbolic tangent can only be small by virtue of δn being very small in our case. Hence we have $R \approx 2(\delta n)^2 K^2 (d/\lambda_3)^2$ and the intensity of the scattered signal $I_3 \propto R \propto (\delta n_e)^2$.

III. RESULTS AND DISCUSSION

The resulting induced coherent Thomson scattering spectral profiles, in relative units, calculated as outlined above are presented in Fig. 2. As checked by direct numerical calculations, the electrostatic electric field E given by (2) is negligible and dropping it from equation (1) does not affect the results presented below. With n_e = 10^{11} cm^{-3} and a numerically established amplitude of electron density perturbation $(\delta n_e)_a/n_e = 1.5\times10^{-2}$ for the high pump intensities assumed here (amplitude of I = 10^{12} W cm^{-2}), the corresponding maximum electric field strength would be 0.013 V cm^{-1}.

For the intensity of the pump beams of $I = 10^9$ Wcm^{-2}, which corresponds to $|U|/(kT_e) = 10^{-4}$, the periodic density perturbation induced on the electrons by the optical lattice is very small. The electron distribution function remains approximately equal to the Maxwellian one. However, as shown on Fig.2a, this weak perturbation provides the broadened Thomson scattering spectral profile, which is 10% wider than the spontaneous scattered profile. This effect is analogous to that predicted and observed in neutral gases [23,32].

With increased pump intensity $I > 10^9$ W cm^{-2}, the obtained spectral profile first begins to narrow and then reaches saturation. The variation of the line shape with the pump intensity is shown in Fig. 2b for the electron temperature T_e= 1 eV, where the considered pump intensity is not higher than 10^{12} W cm^{-2}. The comparison of the spectral lines at I = 10^{11} and 10^{12} W cm^{-2} clearly demonstrates the saturation of the narrowing with pump intensity. Such a narrowing is again similar to that predicted and observed in neutral gases [32,34].

For an increased electron temperature, T_e= 3 eV, we again find the spectral profiles undergoing the saturation of the broadening when decreasing the pump intensity and the

saturation of the narrowing when increasing the pump intensity. The broad and narrow spectra are shown in Fig. 2c.

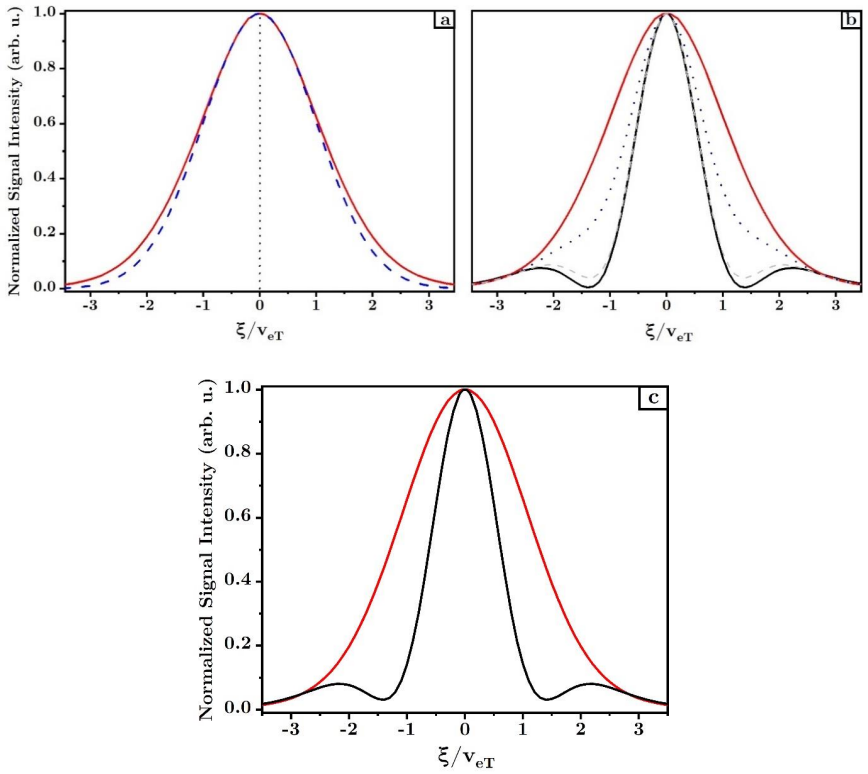

FIG. 2. (a) Induced coherent Thompson scattering spectral profile from an electron gas with temperature T_e = 1 eV at a pump intensity. I = 10^9 W cm^{-2} vs the dimensionless phase velocity of the optical lattice. For comparison, also shown are the Doppler profile of spontaneous Thomson scattering from an electron gas at T_e = 1 eV (dashed blue line) and Doppler profile of spontaneous Rayleigh scattering from neutral argon gas with temperature T= 293 K, as seen at characteristic electron velocities (dotted line). The spontaneous Thomson and Rayleigh scattering profiles are shown as a function of $\xi = \Delta\Omega/h$, where $\Delta\Omega$ is the difference between the incident light wave frequency and the scattered one and $h = |\boldsymbol{k} - \boldsymbol{k}'|$; (b) A comparison between calculated induced coherent Thompson scattering spectral profiles from electron gas with temperature T_e = 1 eV at pump intensities I = 10^9 W·cm^{-2} (red solid line) and I = 10^{12} W·cm^{-2} (black solid line). Also shown are the calculated spectral profiles from the same electron gas at intermediate intensities I = 10^{10} W·cm^{-2} (dotted line) and at I = 10^{11} W·cm^{-2} (dashed line); (c) The same as in (b) but for T_e = 3 eV; I = $3\cdot10^9$ W·cm^{-2} (red solid line) and I = $3\cdot10^{12}$ W·cm^{-2} (black solid line).

Although an analytical theory of the narrowing is not developed yet, qualitatively the effect is related to the trapping of the particles (electrons) within the moving potential [32]. Additionally, we note that the pump intensity I = 10^{12} W cm^{-2} corresponds to

$|U|/(kT_e) = 0.1$. Unlike the case with low pump intensity, at high pump intensity the perturbation of the electron distribution function due to its interaction with the optical lattice is noticeable. As a result, after interaction of the electronic gas with intense optical fields, a plateau forms within the distribution function due to the oscillation of the particles within the potential well. This effect is counteracted by electron-neutral collisions trying to restore the Maxwellian distribution function. The resulting perturbed distribution function is shown in Fig. 3. A significant fraction of the electron distribution function is trapped by the optical potential only when optical lattice velocities are not too high $\xi < 2.5v_{eT}$. For this reason, the calculated saturated spectra of Fig.2(b,c) at the high pump intensity strongly deviates from that found at low intensity, where the trapping effect is negligible (Fig. 2(a)). But at $\xi > 2.5v_{eT}$ the saturated spectrum at the high pump intensity approaches that found at low intensity (Fig.2(b,c)).

.

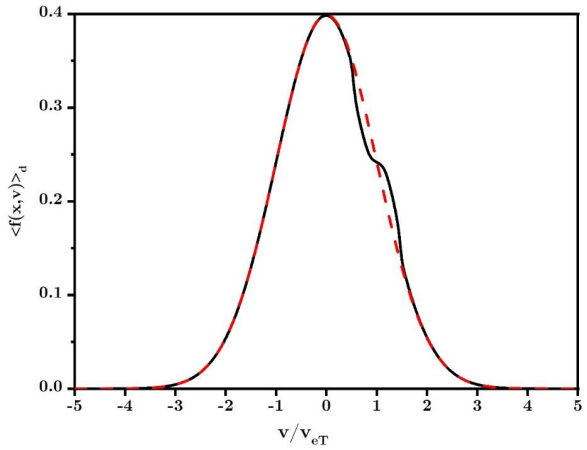

FIG. 3. The steady-state electron velocity distribution function averaged over the optical lattice period, as calculated for the initially unperturbed electron gas placed in an optical lattice moving with velocity ξ = 4.19×10^7 cm s^{-1}. The pump intensity is $I = 10^{12}$ W/cm^2 ; T_e = 1 eV. The dashed line is the initial unperturbed Maxwellian distribution function.

It is expected that a broad Gaussian spectrum at low pump intensities would be difficult to observe, due to the low strength of induced electron density perturbations and the scattered signal. However, the scattered signal should be detectable at higher pump intensities. From the results of Fig. 2, it is observed that the width of the line shape to which

the signal saturates at the high pump intensity is approximately two times lower than that of the Gaussian spectrum.

The width of the Gaussian spectrum is proportional to square root of T_e. The narrow, saturated signal possesses approximately the same property for the above numerical examples with T_e = 1 eV and 3 eV in argon. In these calculations, we took into account the variations of the electron mean free path with T_e , $l=l(T_e)$ through the dependence of the momentum transfer cross section on the electron energy [35]. Let us calculate full-width-at-half-maximum (FWHM) $\Delta\omega=q\xi_{1/2}$ of the narrowed spectra of Fig. 2b and Fig. 2c, where $q = 4\pi/\lambda$ and $\xi_{1/2}$ is FWHM measured in terms of the lattice velocity. For the narrowed spectrum of Fig 2b (black solid line), we have $\xi_{1/2} \approx 1.2v_{eT}$, $v_{eT} = \sqrt{kT_e/m}$, T_e = 1 eV , and $\Delta\omega \approx 1.2\cdot10^{13}$ s^{-1} or $1.9\cdot10^3$ GHz. For the narrowed spectrum of Fig 2c (black solid line), with T_e = 3 eV and $\xi_{1/2} \approx 1.24v_{eT}$ found from this figure, we obtain $\Delta\omega \approx 2.1\cdot10^{13}$ s^{-1} or $3.4\cdot10^3$ GHz. We see that within the accuracy of 3% (the constant 1.2 replaced by 1.24) FWHM is proportional the square root of the electron temperature T_e , $\Delta\omega = q\xi \propto \sqrt{T_e}$.

If it is assumed that $l=l(T_e)$=const, as it is in helium in the considered range of T_e, it would have been obtained that the above dependence of FWHM of the narrowed spectrum on T_e is exact. The reason for this behavior is clear: in the case of a negligible electrostatic field $E \approx 0$, Eq. (1) can be rewritten, introducing the dimensionless variables $\tilde{v} = v/v_{eT}$, $\tilde{x} = x/d$ and $\tilde{t} = tv_{eT}/d$:

$$\frac{\partial \tilde{f}}{\partial \tilde{t}} + \tilde{v}\frac{\partial \tilde{f}}{\partial \tilde{x}} + \frac{F_a d}{m v_{eT}^2}\sin\left[\tilde{q}\left(\frac{\tilde{t}\xi}{v_{eT}} + \tilde{x}\right)\right]\frac{\partial \tilde{f}}{\partial \tilde{v}} = -\sqrt{\frac{8}{\pi}}\frac{d}{l}\left(\tilde{f} - \tilde{f}_0\right) \quad (3)$$

with $\tilde{f}_0 = 1/\left(\sqrt{2\pi}\right)exp\left(-\tilde{v^2}/2\right)$, $\tilde{f} = fv_{eT}$, $\tilde{q} = qd$ and $F_a = \frac{e^2E_0^2q}{2m\omega^2}$ (in the last expression we assume that $E_0 = E_{01} = E_{02}$). Equation (3) shows that if $l = l(T_e) = const$ the solution $\delta f = \int_{-\infty}^{+\infty}(f - f_0)dv = \int_{-\infty}^{+\infty}\left(\tilde{f} - \tilde{f}_0\right)d\tilde{v}$ as a function of ξ/v_{eT} depends only on the value $F_a d/(mv_{eT}^2) \propto I/T_e$. Therefore, with ξ/v_{eT} fixed, the variations in both I and T_e such that the ratio I/T_e remains constant would not change the perturbation δf and thus the calculated signal lies on the universal curve I_s vs. ξ/v_{eT}.

To demonstrate the improvement offered by our approach, let us estimate the intensity of the coherent scattered signal for relatively high pump beam intensities $I_1 = I_2 = I = 10^{12}$ W·cm^{-2} , and probe beam intensity I_3=I. According to the numerical simulations, with these values of I_1 and I_2, the perturbation of the electron density of $n_e = 10^{11}$ cm^{-3} due to the optical lattice is $\delta n_e/n_e \approx 10^{-2}$. For a probe beam with wavelength $\lambda_3 = 532$ nm, this

results in the perturbation of the index of refraction $\delta n = -(\omega_p/\omega_3)^2 \delta n_e/(2n_e) = -1.3 \cdot 10^{-13}$. Assuming a typical length for the optical lattice of $L =$ 1 cm, the number of lattice periods will be $K = 3.8 \times 10^4$ and thus the reflection coefficient $R \approx 1.2 \times 10^{-17}$. Therefore, the intensity of the scattered signal will be $I_4 = R I_3 = 1.2 \times 10^{-5}$ W·cm^{-2}. The number of photons in the reflected signal per a probe laser pulse of a duration δt is $N_{ph} = I_4 \delta t \lambda_3 S/(hc)$, where $S = \pi R_b^2$ is the area of the laser beam and h is Plank's constant. With $\delta t = 5$ ns and $R_b = 100$ μm we have $N_{ph} \approx 50$, which is acceptable for reliable measurements [4]. At the low pump intensities I_1 and $I_2 = 10^9$ W·cm^{-2}, we have the amplitude of perturbations $\delta n_e/n_e \approx 4 \times 10^{-5}$ and the number of photons N_{ph} would be significantly lower.

In case of a standard incoherent Thomson scattering, number of scattered photons N_s is given by [4]

$$N_S \approx \frac{I_3 \delta t \lambda_3}{hc} n_e V r_0^2 \Delta\Omega \eta, \qquad (4)$$

where $V = SL_S$ is the scattering volume, L_S is its length, r_0 is the classical electron radius, $\Delta\Omega$ is the solid angle of observation and η is the transmission coefficient of the optical system. Let us estimate N_s for a typical experimental case. Using the same values of $I_3 = 10^{12}$ W·cm^{-2}, δt= 5 ns, λ_3=532 nm, $n_e = 10^{11}$ cm^{-3}, $S=\pi R_b^2$, R_b=100 μm, and L_S= 1 cm as we have taken above in evaluating N_{ph} for the coherent scattering, substituting r_0 = 2.82×10^{-13} cm, and assuming $\Delta\Omega$=10^{-3} sr and η =0.1 as in [4], we obtain $N_s \approx 3$. Comparing this value with $N_{ph} \approx 50$ estimated for the coherent Thomson scattering, we can conclude that the proposed coherent Thomson scattering technique can be preferable to a standard incoherent Thomson scattering technique for diagnostics of low-temperature plasma sources.

CONCLUSION

At the core of the proposed four-wave mixing Thomson scattering scheme is the utilization of optical lattices for the creation of the periodic perturbation of electron density in plasmas via a periodic optical dipole force. The traveling optical potential perturbs the motion of a group of electrons whose velocities are close to the speed of the interference pattern of the crossed pump fields. By changing the frequency difference between the two pump laser beams, or the speed of the interference pattern, a perturbation of electron distribution function centered at the particular velocity is created. The relative magnitude of the induced electron density perturbation at each velocity can be determined by the measurement of the relative

intensity of a third probe laser beam, Bragg scattered from the induced electron density perturbations.

This scheme is capable of by-passing the Rayleigh signal contributions from neutrals and ions in the plasma - only keeping the Thomson scattering signal from the electrons. More importantly, this scheme results in a coherent Thomson signal beam, which maintains all the beam characteristics of the probe beam. This enables the placement of the collection optics far from the point of measurement without any loss of signal, in comparison to e.g. incoherent Thomson scattering where the signal scales with $1/r^2$ with respect to the distance r where the collection optics are placed. It is envisioned that this capability will enable accurate and non-intrusive measurements in low density plasmas, where the current state-of-the-art is mechanical probes.

The four-wave mixing nature of the proposed technique renders it ideal for application in optically noisy environments, such as those encountered in plasmas - while the necessary angled crossing of the laser beams provides with a high degree of localization and spatial resolution. Furthermore, if one utilizes a chirped lattice approach, where the range of optical lattice velocities is scanned in a single laser shot (as experimentally demonstrated and theoretically studied for neutral gases in Ref. [25]), it is envisioned that the induced coherent Thomson scattering scheme will have single shot spectral acquisition, making it an ideal diagnostic for highly dynamic systems.

ACKNOWLEGMENTS

This work is partially supported by the Princeton Collaborative Research Facility (PCRF), supported by the U.S. Department of Energy (DOE) under Contract No. DE-AC02-09CH11466. A.G. also received support from the U.S. DOE Office of Science Award No. DE- SC0021183.

DATA AVAILABILITY

The data that support the findings of this study are available from the corresponding author upon reasonable request.

REFERENCES

[1] P. C. Clemmow and J. P. Dougherty, *Electrodynamics of Particles and Plasmas* (Addison—Wesley series in Advanced Physics, 1969).
[2] J. Sheffield, D. Froula, S. H. Glenzer, and N. C. Luhmann Jr, *Plasma Scattering of Electromagnetic Radiation: Theory and Measurement Techniques* (Academic press, 2010).
[3] N. J. Peacock, D. C. Robinson, M. J. Forrest, P. D. Wilcock, and V. V. Sannikov, *Measurement of the Electron Temperature by Thomson Scattering in Tokamak T3*, Nature **224**, 488 (1969).
[4] K. Muraoka and A. Kono, *Laser Thomson Scattering for Low-Temperature Plasmas*, J. Phys. D. Appl. Phys. **44**, 43001 (2011).
[5] S. Yip and M. Nelkin, *Application of a Kinetic Model to Time-Dependent Density Correlations in Fluids*, Phys. Rev. **135**, A1241 (1964).
[6] H. J. Van Der Meiden, S. K. Varshney, C. J. Barth, T. Oyevaar, R. Jaspers, A. J. H. Donń, M. Y. Kantor, D. V. Kouprienko, E. Uzgel, W. Biel, and A. Pospieszczyk, *10 KHz Repetitive High-Resolution TV Thomson Scattering on TEXTOR: Design and Performance (Invited)*, Rev. Sci. Instrum. **77**, (2006).
[7] M. Y. Kantor, A. J. H. Donné, R. Jaspers, and H. J. van der Meiden, *Thomson Scattering System on the {TEXTOR} Tokamak Using a Multi-Pass Laser Beam Configuration*, Plasma Phys. Control. Fusion **51**, 55002 (2009).
[8] L. A. Berni and B. F. C. Albuquerque, *Stray Light Analysis for the Thomson Scattering Diagnostic of the ETE Tokamak*, Rev. Sci. Instrum. **81**, 123504 (2010).
[9] X. Han, C. Shao, X. Xi, J. Zhao, Z. Qing, J. Yang, X. Dai, and K. Shinichiro, *Data Processing and Analysis of the Imaging Thomson Scattering Diagnostic System on HT-7 Tokamak*, Rev. Sci. Instrum. **84**, 053502 (2013).
[10] D. Feng, A. Diallo, and M. N. Shneider, *Two-Color Scattering for the Measurement of Neutrals at the Edge of Fusion Devices*, Rev. Sci. Instrum. **92**, 63515 (2021).
[11] K. Muraoka, K. Uchino, and M. D. Bowden, *Diagnostics of Low-Density Glow Discharge Plasmas Using Thomson Scattering*, Plasma Phys. Control. Fusion **40**, 1221 (1998).
[12] C. Jiang, J. Miles, J. Hornef, C. Carter, and S. Adams, *Electron Densities and Temperatures of an Atmospheric-Pressure Nanosecond Pulsed Helium Plasma Jet in Air*, Plasma Sources Sci. Technol. **28**, 085009 (2019).
[13] S. Hübner, J. S. Sousa, J. Van Der Mullen, and W. G. Graham, *Thomson Scattering on Non-Thermal Atmospheric Pressure Plasma Jets*, Plasma Sources Sci. Technol. **24**, 054005 (2015).
[14] A. Roettgen, I. Shkurenkov, M. Simeni Simeni, V. Petrishchev, I. V. Adamovich, and W. R. Lempert, *Time-Resolved Electron Density and Electron Temperature Measurements in Nanosecond Pulse Discharges in Helium*, Plasma Sources Sci. Technol. **25**, 055009 (2016).
[15] S. Maurmann, V. A. Kadetov, A. A. I. Khalil, H. J. Kunze, and U. Czarnetzki, *Thomson Scattering in Low Temperature Helium Plasmas of a Magnetic Multipole Plasma Source*, J. Phys. D. Appl. Phys. **37**, 2677 (2004).
[16] D. L. Crintea, U. Czarnetzki, S. Iordanova, I. Koleva, and D. Luggenhölscher, *Plasma Diagnostics by Optical Emission Spectroscopy on Argon and Comparison with Thomson Scattering*, J. Phys. D. Appl. Phys. **42**, 045208 (2009).
[17] B. Vincent, S. Tsikata, S. Mazouffre, T. Minea, and J. Fils, *A Compact New Incoherent Thomson Scattering Diagnostic for Low-Temperature Plasma Studies*, Plasma Sources

Sci. Technol. **27**, 55002 (2018).
[18] M. N. Shneider, *Ponderomotive Perturbations of Low Density Low-Temperature Plasma under Laser Thomson Scattering Diagnostics*, Phys. Plasmas **24**, 100701 (2017).
[19] S. Tsikata, N. Lemoine, V. Pisarev, and D. M. Grésillon, *Dispersion Relations of Electron Density Fluctuations in a Hall Thruster Plasma, Observed by Collective Light Scattering*, Phys. Plasmas **16**, 33506 (2009).
[20] S. Tsikata, J. Cavalier, A. Héron, C. Honoré, N. Lemoine, D. Grésillon, and D. Coulette, *An Axially Propagating Two-Stream Instability in the Hall Thruster Plasma*, Phys. Plasmas **21**, 72116 (2014).
[21] N. M. Kroll, A. Ron, and N. Rostoker, *Optical Mixing as a Plasma Density Probe*, Phys. Rev. Lett. **13**, 83 (1964).
[22] P. Michel, W. Rozmus, E. A. Williams, L. Divol, R. L. Berger, S. H. Glenzer, and D. A. Callahan, *Saturation of Multi-Laser Beams Laser-Plasma Instabilities from Stochastic Ion Heating*, Phys. Plasmas **20**, 056308 (2013).
[23] J. H. Grinstead and P. F. Barker, *Coherent Rayleigh Scattering*, Phys. Rev. Lett. **85**, 1222 (2000).
[24] X. Pan, M. N. Shneider, and R. B. Miles, *Coherent Rayleigh-Brillouin Scattering*, Phys. Rev. Lett. **89**, 183001 (2002).
[25] A. Gerakis, M. N. Shneider, and P. F. Barker, *Single-Shot Coherent Rayleigh–Brillouin Scattering Using a Chirped Optical Lattice*, Opt. Lett. **38**, 4449 (2013).
[26] A. Gerakis, M. N. Shneider, and P. F. Barker, *Coherent Brillouin Scattering*, Opt. Express **19**, 24046 (2011).
[27] H. Batelaan, *Colloquium: Illuminating the Kapitza-Dirac Effect with Electron Matter Optics*, Rev. Mod. Phys. **79**, 929 (2007).
[28] P. L. Bhatnagar, E. P. Gross, and M. Krook, *A Model for Collision Processes in Gases. I. Small Amplitude Processes in Charged and Neutral One-Component Systems*, Phys. Rev. **94**, 511 (1954).
[29] R. J. LeVeque, *Finite Volume Methods for Hyperbolic Problems* (Cambridge University Press, 2002).
[30] R. B. Horne and M. P. Freeman, *A New Code for Electrostatic Simulation by Numerical Integration of the Vlasov and Ampère Equations Using MacCormack's Method*, J. Comput. Phys. **171**, 182 (2001).
[31] M. N. Shneider and P. F. Barker, *Optical Landau Damping*, Phys. Rev. A **71**, 053403 (2005).
[32] H. T. Bookey, M. N. Shneider, and P. F. Barker, *Spectral Narrowing in Coherent Rayleigh Scattering*, Phys. Rev. Lett. **99**, 133001 (2007).
[33] A. Yariv and P. Yeh, *Optical Waves in Crystals*, Vol. 5 (Wiley New York, 1984).
[34] M. N. Shneider, P. F. Barker, X. Pan, and R. B. Miles, *Coherent Rayleigh Scattering in the High Intensity Regime*, Opt. Commun. **239**, 205 (2004).
[35] Phelps database, www.lxcat.net, retrieved on November 21, 2021.
C. Yamabe, S. J. Buckman, and A. V. Phelps, Measurement of free-free emission from low-energy-electron collisions with Ar, Phys. Rev. A 27, 1345 (1983).